Estimation of Depth to Basement within Sokoto Basin for Hydrocarbon Exploration using High Resolution Aeromagnetic Data by Spectral Analysis

M. Abbas[1], A. Jimoh[1], D.S. Bonde[1], C.M. Elinge[2]

1. *Department of Physics, Faculty of physical Sciences, Kebbi State University of Science And Technology, Aleiro Kebbi State, Nigeria.*
2. *Department of Chemistry, Faculty of physical Sciences, Kebbi State University of Science And Technology, Aleiro Kebbi State, Nigeria.*

ABSTRACT
This study presents the analysis and interpretation of aeromagnetic data over part of Sokoto Basin with the aim of investigating the hydrocarbon potentials of the study area. The study area is located between latitudes $12^{0}00''$N and $13^{0}.50''$N and longitudes $4^{0}.00''$E and $7^{0}.00''$E. The total magnetic intensity map was subjected to regional/residual separation. The spectral analysis technique was used to estimate the sediment thickness of the study area. The results of the analysis of high resolution aeromagnetic data show that, deeper magnetic sources for the technique are 2.27 km and the shallow magnetic source is 0.4 km respectively. The results indicate an increase in sedimentation northwards, with several depressions on the basement rock. The areas, where higher sedimentary thicknesses are observed are observed such as block 26, block.27 and block 28 with 2.26 km, 2.10 km and 2.27 km thickness of sediments respectively, is the most probable sites for prospect of hydrocarbon accumulation in the study area of Sokoto Basin. The maximum sedimentary thickness of 2.27 km in the study area is not sufficient for sufficient for hydrocarbon maturation and accumulation. The implication of these results is that, even if all other conditions are met, the possibility of hydrocarbon exploration and exploitation in the basin may be very marginal.
KEY WORDS: Hydrocarbon Potentials, High Resolution Aeromagnetic Data, Spectral Analysis, Sokoto Basin, Nigeria

I. INTRODUCTION

Hydrocarbon resources have always been important and essential natural resources to the general economic development of different countries in the world. There is need to sustain the production of these resources, so as to maintain and improve the general standard of living within these countries. Owning to the fact that, there is high cost incurred in the exploration of these vital resources. It is very important to achieve maximum perfection in its detection and analysis for its quantification. Since cost effectiveness is one of the major challenging factors in the oil and gas industry, hydrocarbon exploration, reservoir interpretation and analysis should be thoroughly subjected to the best available technology to achieve the lowest level of uncertainty in its exploration and production.

The earth and its contents have long been of concern to mankind. Man has tried to unravel its complexity and delve into its origin via various geophysical methods. The subsurface has been of particular concern to geoscientists, who seek to investigate it using diverse means, some for the purpose of having knowledge, while others do it for exploration of economic resources such as minerals and hydrocarbons. Geophysics involves the application of physical principles and quantitative physical measurements in order to study the earth's interior, its atmosphere, and terrestrial space. The analysis of these measurements can reveal how the earth interior varies both vertically and laterally, and the interpretation of which can reveal meaningful information on the geological structures beneath (Dobrin, 1976).

Aeromagnetic survey technique is a notable geophysical method which has been used effectively to investigate subsurface geology in different capacity such as archeological,

geothermal, hydrocarbon and mineral studies. Studies of aeromagnetic data with interest in hydrocarbon exploration have been performed in recent years. The study that employed aeromagnetic data of Muglad Basin in South Sudan discovered magnetic anomalies which clustered along a prospective structure and coincided with the Jarayan oil field. A major advantage of aeromagnetic survey is the accessibility to cover major inaccessible areas that might prove expensive and slower to map out. For hydrocarbon resources, the aeromagnetic surveys are used at the initial stages to map out and evaluate the thickness of the sedimentary basin. This is achievable by analyzing and estimating the depths of the magnetic sources (i.e. the magnetic basement rocks

causing the observed anomalies) within the study area. Largely, this is subjected to the fact that sedimentary rocks are non-magnetic for all intents and purpose. Therefore, the aeromagnetic anomaly is attributed to basement rocks.

1.1 Location and the Geological Settings of the Study Area

The study area falls within Sokoto Basin, Northwestern Part of Nigeria which comprises of 18 sheets with 50 local governments areas of three states (Sokoto, Kebbi and Zamfara States) in the Northwestern Nigeria as shown in Fig 1. They are bounded by longitudes 4.00^0E to 7.00^0E and latitudes 12.00^0N to 13.50^0N in the Northwestern Nigeria.
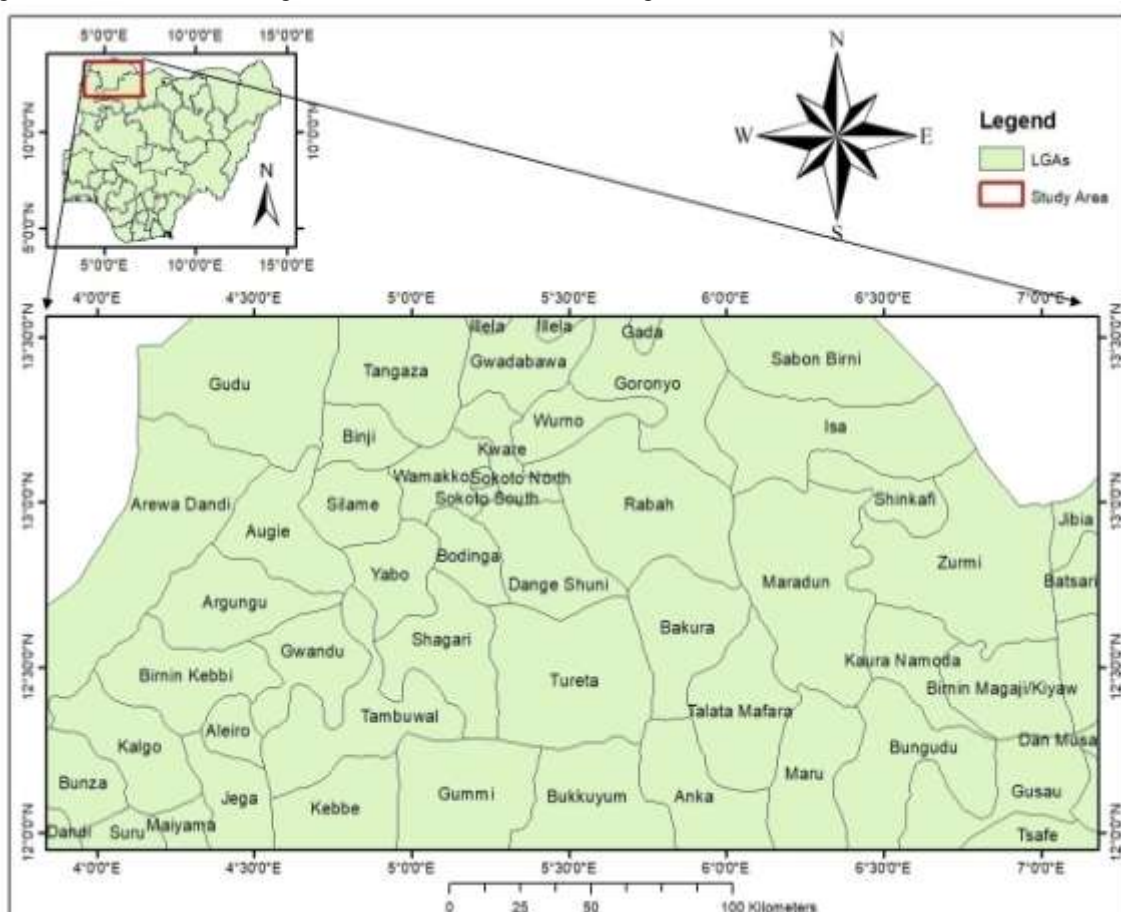

Fig 1. Location Map of the Study Area

1.2 Geology of the Study Area

The geology of the Sokoto Basin has been greatly explained by different scholars, such as Obaje 2009; Kogbe. 1976; the Sokoto Basin was extensively explained by Obaje et al 2013. The sediments of the Iullemmeden Basin were accumulated during four main phases of deposition.

Overlying the Pre-Cambrian Basement unconformably, the Illo and Gundumi Formations, made up of grits and clays, constitute the Pre-Maastrichtian "**Continental Intercalaire**" of West Africa. They are overlain unconformably by the Maastrichtian **Rima Group**, consisting of mudstones and friable sandstones (Taloka and

Wurno Formations), separated by the fossiliferous, calcareous and shaley Dukamaje Formation. The Dange and Gamba Formations (mainly shales) separated by the calcareous Kalambaina Formation constitute the Paleocene **Sokoto Group**. The overlying continental Gwandu Formation forms the Eocene **Continental Terminal**. These sediments dip gently and thicken gradually towards the northwest with maximum thicknesses attainable toward the border with Niger Republic.

The "Continental Intercalaire" is important in Africa. The Karoo Series of South Africa can be correlated with the upper beds of the lower portion of the Continental Intercalaire group. The Continental Intercalaire group corresponds to the upper part of the Nubian Sandstone, which, in

the Arabo-Nubian shield, begins at the base of the Palaeozoic. The Iullemmeden Basin, as well as many other parts of North and South Africa, experienced extensive periods of continental sedimentation with the accumulation of fluvio-lacustrine sediments in pre-Cenomanian times. The northern limits of the continental deposition coincides with the Algeria- Moroccan Sahara and extends eastward into Egypt and the Sudan. The southern limits extend as far as South Africa. However, the study area has five geological formations namely; Gwandu formation, Wurno formation, Dukamaje formation, Taloka formation and Ilo/Gundumi formation as shown in the Figure 2.
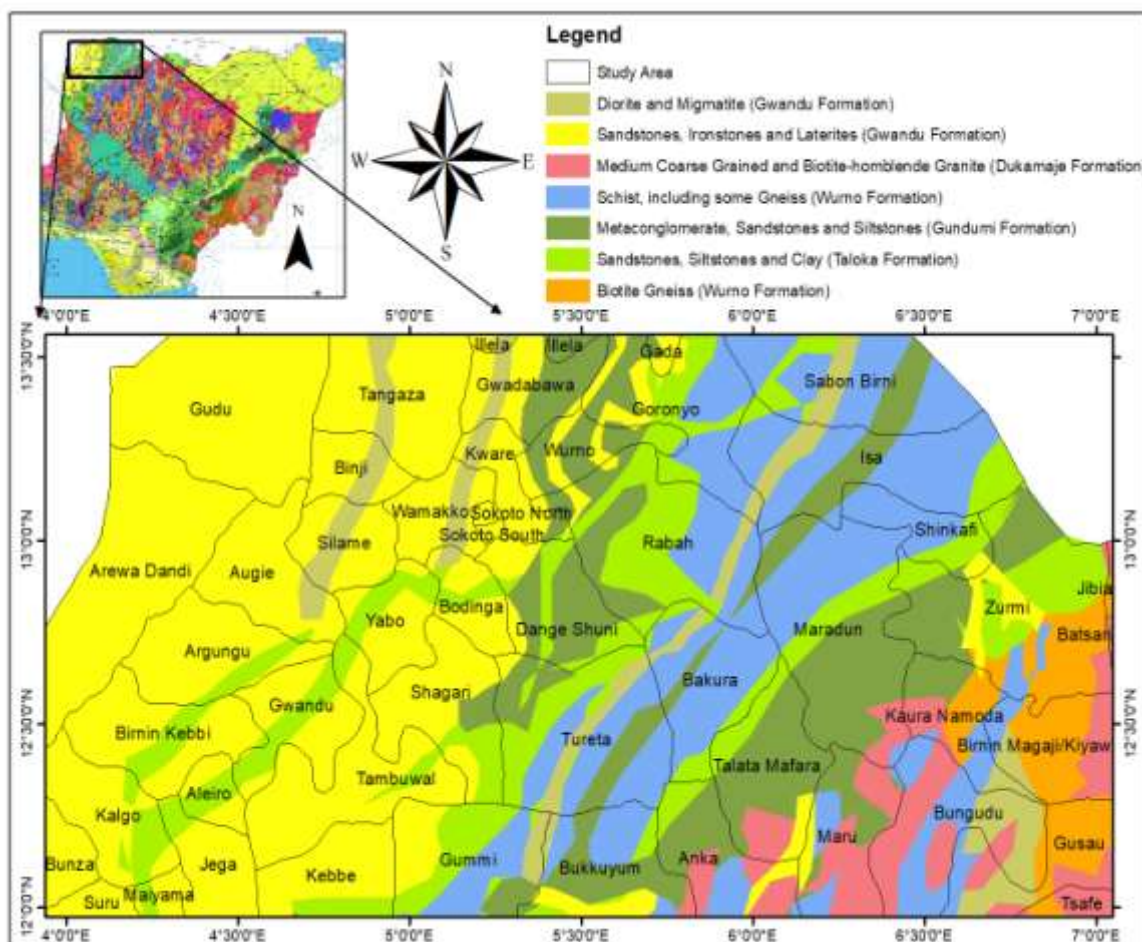

Fig 2. The Geological Map of the Study Area.

II. MATERIALS AND METHOD
2.1 Data acquisition

Eighteen (18) half degree by half degree airborne radiometric data were acquired from the Nigerian Geological Survey Agency (NGSA) Abuja. The sheet numbers with their respective

locations are; Sheet 8(Sakkwabe), Sheet 9(Binji), sheet 10(Sokoto), Sheet 11(Rabah), sheet 12(Isah), Sheet 13(Shinkafe), sheet 27(Leman), sheet 28(Arugungu), sheet 29(Dange), sheet 30(Gandi), sheet 31(Mafara), sheet 32(Kaura), sheet 49(Birnin Kebbi), sheet 50(Tambuwa), sheet 51(Gunmi),

sheet 52(Ankah), sheet 53(Maru), and sheet 54(Gusau). The aero-radiometric dataset was obtained as part of the airborne survey carried out between 2005 and 2009 by Fugro on behalf of the Nigerian Geological Survey Agency. The data were obtained at an altitude of 100 m along with a flight line spacing of 500 m oriented in NW-SE and a tie line spacing of 2000 m. The maps are on a scale of 1:100,000 and half-degree sheets.

2.2. Methods
2.2.1 Regional-Residual Separation
The total magnetic field intensity is made up of two parts: the regional field and the residual field. Values of the regional fields are always very high when compared to that of the residual fields and most often shields or masks the residual fields thereby making their effects generally unnoticed. In interpreting aeromagnetic data, an attempt is made at separating the higher frequency regional fields from the low frequency residual fields. In doing this the method used is often by fitting a plane surface to the total field data. Therefore, generally speaking, regional – residual separation is carried out by polynomial fitting using multiple regression analysis. Subtraction of the calculated (regional) values from that of the original magnetic field intensity values gives the residual values.

2.2.2 Production of Regional and Residual Maps
The residual magnetic field of the study area was produced by subtracting the regional field from the total magnetic field using the Polynomial fitting method. The computer program Aerosupermap was used to generate the coordinates of the total intensity field data values. This super data file, for all the magnetic values was used for production of composite aeromagnetic map of the study area using Oasis Montaj software version 8.3. A program was used to derive the residual magnetic values by subtracting values of regional field from the total magnetic field values to produce the residual magnetic map and the regional map.

2.2.3 Spectral Depth Analysis Method:
It is a depth estimating method used in geophysics for investigating the thermal frame work via aeromagnetic studies. Spectral depth analysis based on statistical models has been employed in numerous geophysical works, as in the determination of average depth to the top of magnetic basement and in the computation of crustal thickness. The Fourier transform of the potential filed due to a prismatic body has a broad spectrum whose peak location is a function of the depth to the top and bottom surfaces and whose amplitude is determined by its density or magnetization (Adetona and Abu, 2013). The expression below shows the relation of the peak wavenumber to the geometry body (Spector and Grant, 1970):

$$\omega' = \frac{\ln\left(h_b / h_t\right)}{h_b - h_t} \quad \dots\dots\dots\dots\dots\dots(1)$$

where ω' is the peak wave number in radian / ground – unit, h_t the depth to the top and h_b is the depth to the bottom.

$$f(\omega) = e^{-h\omega} \quad \dots\dots\dots\dots\dots\dots(2)$$

where ω is the angular wave number in radians/ground-unit and h is the depth to the top of the prism. For a prism with top and bottom surface, the spectrum is:

$$f(\omega) = e^{-h_t\omega} - e^{-h_b\omega}\dots\dots\dots\dots\dots(3)$$

where h_t and h_b are the depths to top and bottom surface respectively.

$$\text{Log } E(k) = 4\pi hk \dots\dots\dots\dots\dots\dots\dots\dots\dots\dots\dots\dots\dots\dots\dots\dots\dots....(4)$$

Where h is the depth in ground – units and k is the wavenumber in cycles / ground – unit. You can determine the depth of an "ensemble" source can be determined by measuring the slope (m) of the energy (power) spectrum and dividing by 4π. i.e.

$$h = m/4\pi\dots\dots\dots\dots\dots\dots\dots\dots(5)$$

A typical energy spectrum for magnetic data may exhibit three parts—a deep source component, a shallow source component, and a noise component. The thickness of sediments of the study area for hydrocarbon maturation and accumulation would be estimated from the spectral analysis of the aeromagnetic data of the study area. The Fig.3 below is the aeromagnetic sheets which depict the coordinates, the names and the respective sheet numbers of the study area of Sokoto basin.

Fig 3. Aeromagnetic sheets of the study area

III. RESULTS AND DISCUSSION

Digitized airborne magnetometer survey maps of total magnetic field intensity for 18 sheets of the study area in Sokoto basin were acquired, assembled and interpreted. The total magnetic field intensity map derived from the data digitization and enhancement is presented as total magnetic intensity map, regional map, residual map, upward continuation maps of different depths, depth contour map and 3-D surface map respectively (Figures 4-9). The resultant total magnetic field map obtained from the digitized aeromagnetic data shows a very complex pattern of magnetic anomalies of both short and long wavelengths. The total magnetic intensity map of the study area is shown in Fig. 4; the map can be divided in to three main sections though there are others minor depressions scattered all over the area. The low magnetic intensity value represented by dark green – blue color is found all around most areas in the map but concentrated toward the eastern and southeastern parts of the study area, ranging between -58.0 to 55.2 nT. The high magnetic intensity value represented by pink – red color scattered all over the study area but concentrated in the southwestern, northwestern and also little fragments in the northeastern parts of the study area with values varying between 79.2 to 120.6 nT, while the two sections are separated by a zone characterized by medium magnetic intensity value of (57.5 – 77.1 nT) and it is also represented by yellow- orange color with concentration towards central part of the study area.
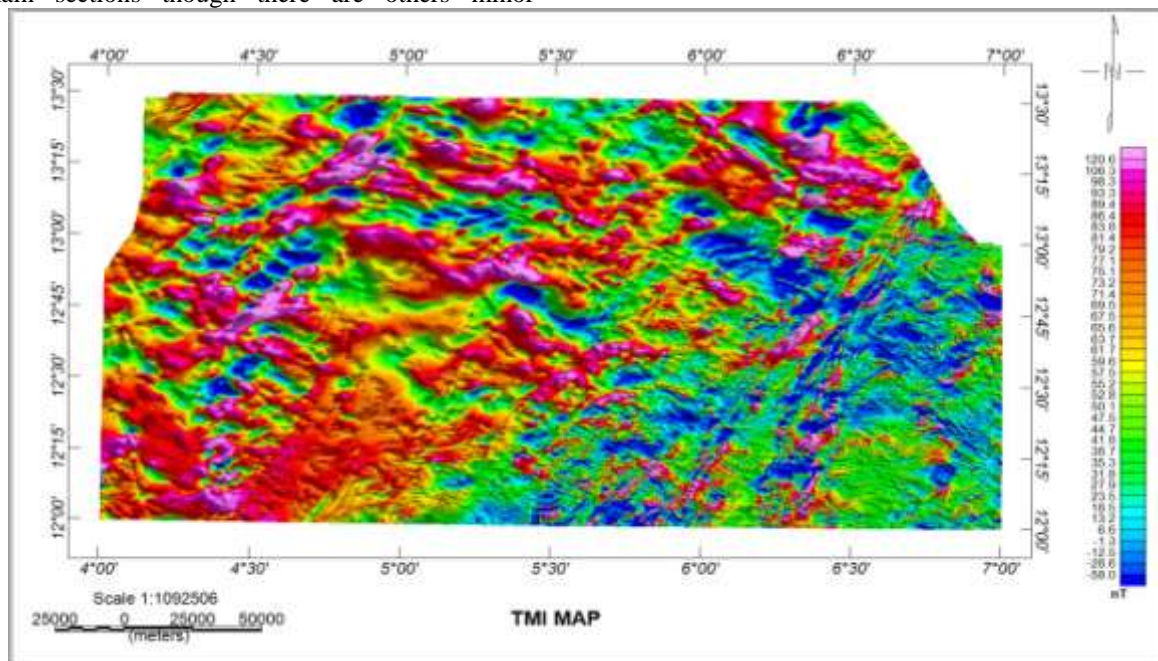

Fig 4. The Total Magnetic Intensity Map of the Study Area

3.1 Regional magnetic intensity map

The regional magnetic values range from 24.2 to 67.2 nT, and the values increase from south to north which depicts that there is a fill of sediments more in the northern part of the basin than in the southern part of the study area.
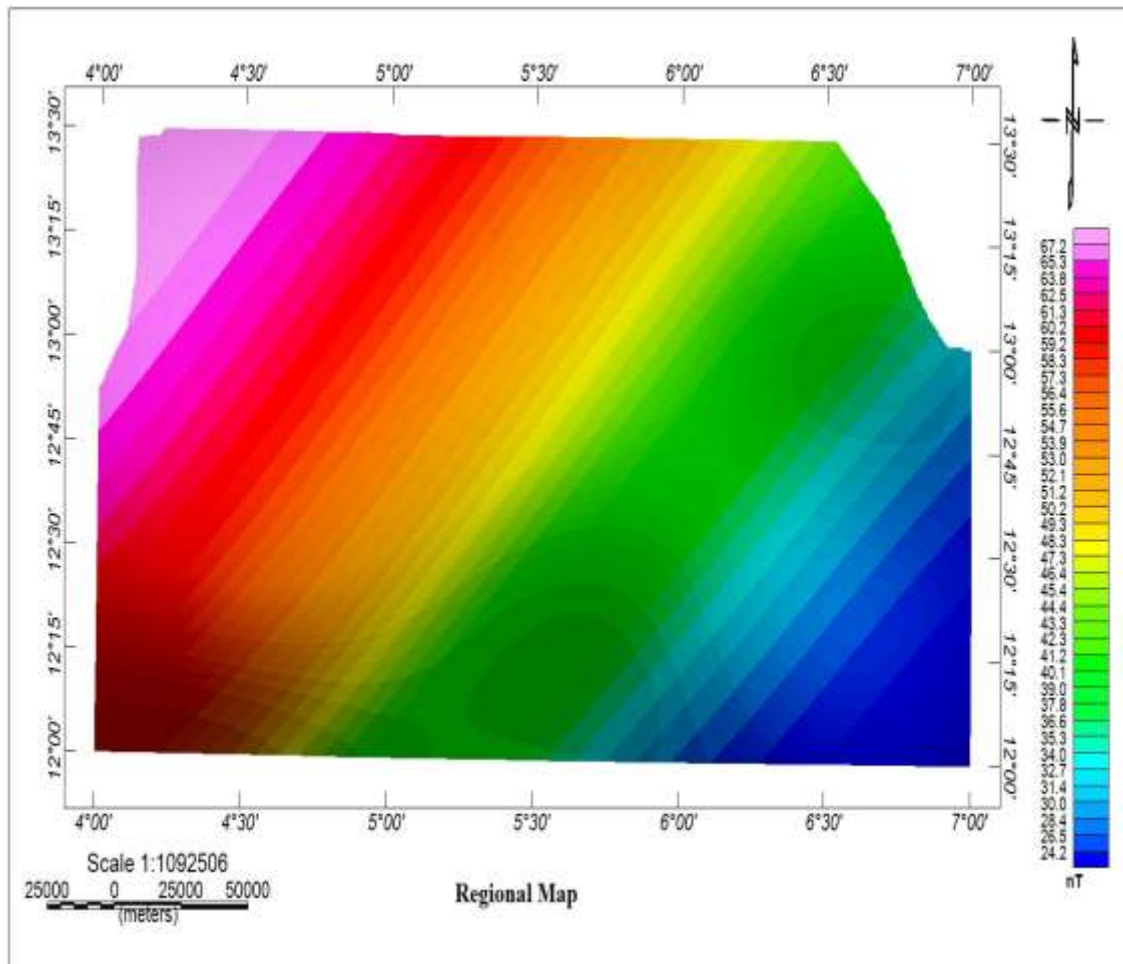

Fig 5. The Regional Magnetic Intensity Map of the Study Area

3.2. Residual Magnetic Intensity Map

Fig.6 is the residual magnetic intensity map of the study area obtained from the total magnetic intensity map produced using Oasis Montaj version 8.3.The residual magnetic map shows magnetic anomalies with high magnetic intensity is represented with pink-red colour which scattered all over the study area but trending to be more prominent in the northern and western parts with values ranging from 24.6 nT to 69.5 nT and a low magnetic intensity is represented with blue-dark green colour which scattered all over the study area but more prominent in the south eastern part of the area with value ranging from -95.7 to 3.2 nT, while the section separating the two is medium magnetic intensity which is represented with yellow-orange colour and also scattered all over the study area but more prominent in the central part of the area with value ranging from 4.9 - 22.3 nT.
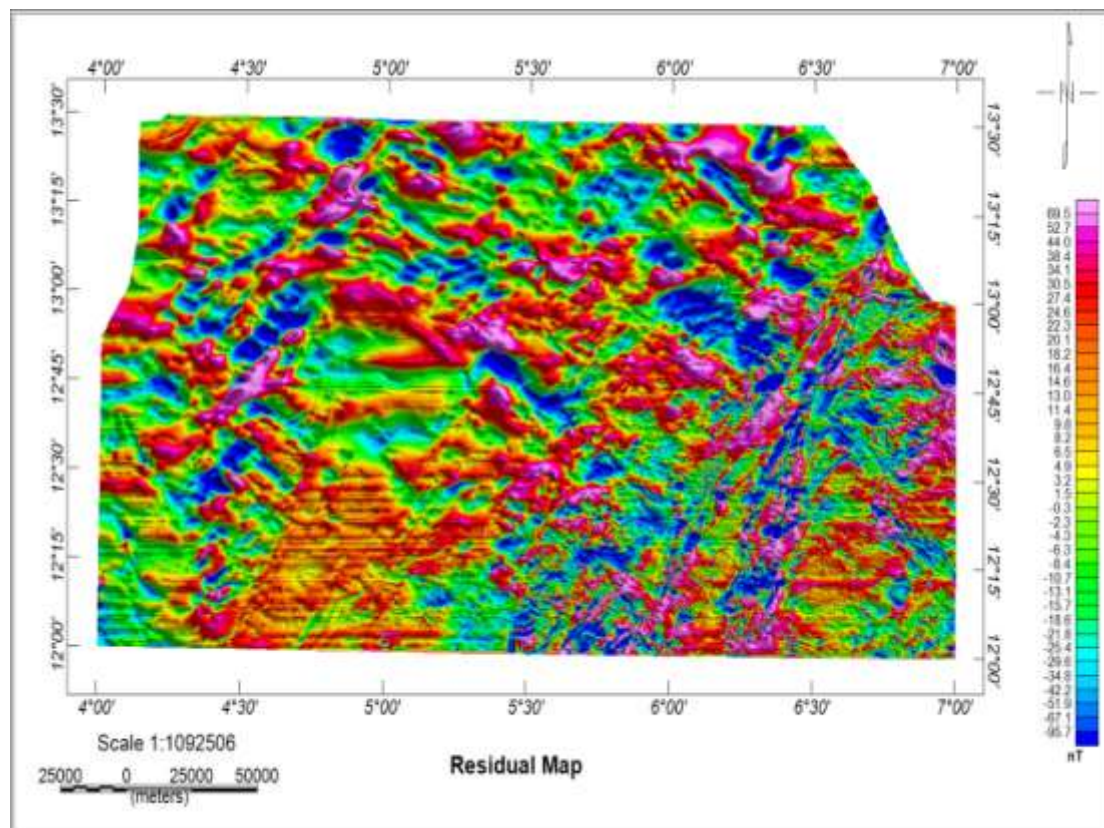
Fig 6. The Residual Magnetic Intensity Map of the Study Area

3.3 Results from the Spectral Analysis

This method was used in this present study to determine the depth to top of magnetic basement based on a moving data window by selecting the sharpest and therefore deepest straight-line segment of the power spectrum. A depth solution was calculated for the power spectrum derived from each grid sub-set located at the centre of the window. Overlapping the windows creates a regular, comprehensive set of depth estimates. The residual map (Figure 6) of the study area was divided into fifty five (55) overlapping spectral blocks (1-55). Spectral analysis was performed on each block and a plot of spectrum energy against wave number was carried out using a program designed with Matlab software. The gradients from the plots give two depths; deeper and shallow depth and the results depth estimated are displayed on Table 1. The deeper depth obtained ranges from 0.48 km to 2.27 km with the maximum depth of 2.27 km found at the north-western part of the study area (Fig. 7a). While the shallow depth ranges 0.12 km to 0.40 km and the shallowest depth could be found at the south-eastern part of the study area (Fig. 7b).
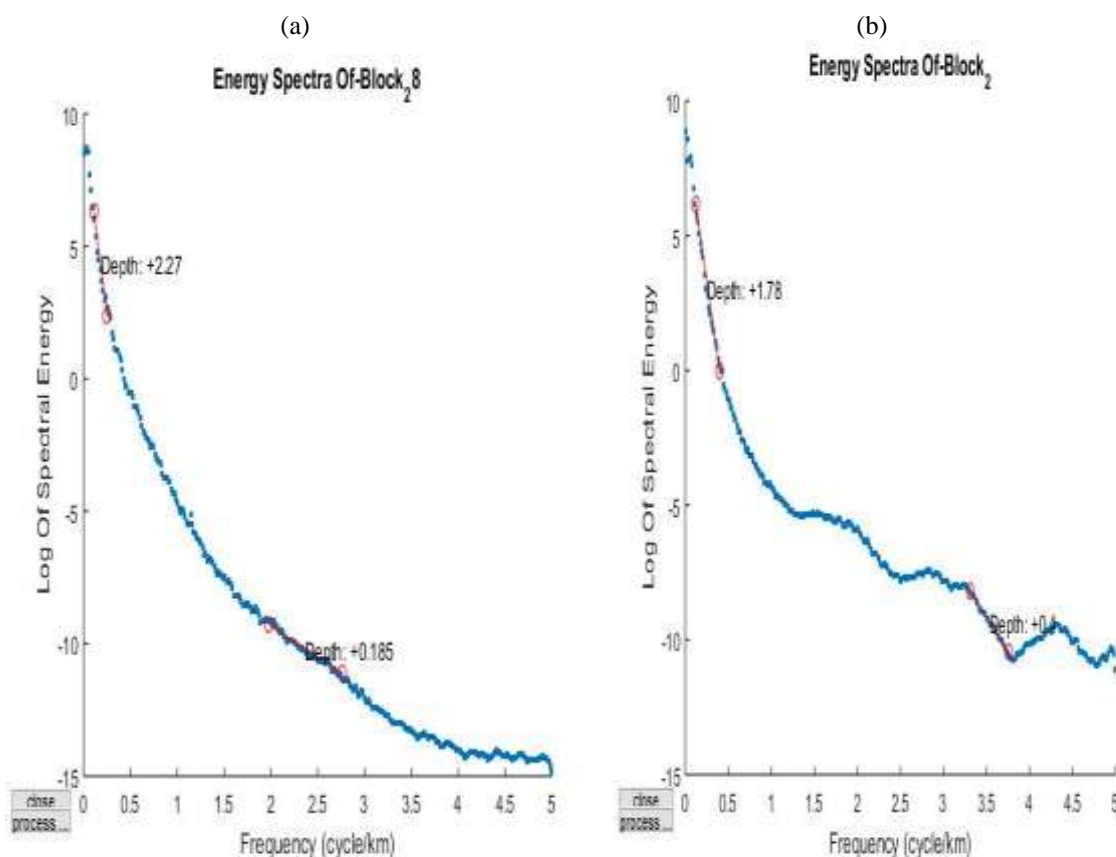
(a)　　　　　　　　　　　　　　　　　　(b)

Fig. 7a & 7b depict the Graphs of spectral plots 28 & 2　　showing the deeper and the shallow depths of the study area

**Table 1. Spectral table of deeper and shallow depth (km) of the study area**

BLOCKS	Long (Deg.)	Lat. (Deg.)	DEEPER DEPTH Z_1 (km)	SHALLOW DEPTH Z_2 (km)
BLOCK 1	4.50	13.50	1.75	0.38
BLOCK 2	4.75	13.50	1.78	0.40
BLOCK 3	5.00	13.50	1.97	0.13
BLOCK 4	s5.25	13.50	1.67	0.18
BLOCK 5	5.50	13.50	1.73	0.13
BLOCK 6	5.75	13.50	1.65	0.21
BLOCK 7	6.00	13.50	1.61	0.26
BLOCK 8	6.25	13.50	1.53	0.21
BLOCK 9	6.50	13.50	1.76	0.29
BLOCK 10	6.75	13.50	1.66	0.27
BLOCK 11	7.00	13.50	1.89	0.29
BLOCK 12	4.50	13.25	1.65	0.15
BLOCK 13	4.75	13.25	1.70	0.15
BLOCK 14	5.00	13.25	1.85	0.21
BLOCK 15	5.25	13.25	1.67	0.22
BLOCK 16	5.50	13.25	1.97	0.37
BLOCK 17	5.75	13.25	2.05	0.23
BLOCK 18	6.00	13.25	1.72	0.25
BLOCK 19	6.25	13.25	1.43	0.32

BLOCK 20	6.50	13.25	1.23	0.23
BLOCK 21	6.75	13.25	0.65	0.34
BLOCK 22	7.00	13.25	0.54	0.32
BLOCK 23	4.50	13.00	1.54	0.19
BLOCK 24	4.75	13.00	1.73	0.18
BLOCK 25	5.00	13.00	1.84	0.18
BLOCK 26	5.25	13.00	2.26	0.29
BLOCK 27	5.50	13.00	2.10	0.19
BLOCK 28	5.75	13.00	2.27	0.19
BLOCK 29	6.00	13.00	1.06	0.22
BLOCK 30	6.25	13.00	1.06	0.24
BLOCK 31	6.50	13.00	0.99	0.35
BLOCK 32	6.75	13.00	0.60	0.36
BLOCK 33	7.00	13.00	0.50	0.37
BLOCK 34	4.50	12.75	1.71	0.24
BLOCK 35	4.75	12.75	1.35	0.19
BLOCK 36	5.00	12.75	1.41	0.16
BLOCK 37	5.25	12.75	1.14	0.31
BLOCK 38	5.50	12.75	1.40	0.28
BLOCK 39	5.75	12.75	1.22	0.35
BLOCK 40	6.00	12.75	1.16	0.33
BLOCK 41	6.25	12.75	0.77	0.34
BLOCK 42	6.50	12.75	0.56	0.38
BLOCK 43	6.75	12.75	0.58	0.38
BLOCK 44	7.00	12.75	0.57	0.38
BLOCK 45	4.50	12.25	1.28	0.21
BLOCK 46	4.75	12.25	0.91	0.19
BLOCK 47	5.00	12.25	0.55	0.33
BLOCK 48	5.25	12.25	0.50	0.12
BLOCK 49	5.50	12.25	0.72	0.32
BLOCK 50	5.75	12.25	0.56	0.39
BLOCK 51	6.00	12.25	0.52	0.34
BLOCK 52	6.25	12.25	0.53	0.37
BLOCK 53	6.50	12.25	0.48	0.39
BLOCK 54	6.75	12.25	0.48	0.35
BLOCK 55	7.00	12.25	0.71	0.38

3.3.1 The contour map of the depth to magnetic basement Z_1 of the study area (contour in km)

The contour of basement depth (Z_1) of the study area is as shown in Figure 8. The depth contour map depicts a number of basement depressions over the entire study area. The depth values suggest that the magnetic basement surface beneath the Sokoto sedimentary basin is generally shallow and of low relief. Depths to magnetic basement range from 0.48 km in the southern and southeastern parts to 2.27 km at the northwestern and a small portion in the northeastern part of the study area, bordering with Niger republic. A closer observation indicates a general increase in thickness from the southern part to northern part, more especially the northwestern part bordering with Niger republic. This general trend in sedimentation implies that the Iullemmenden basin is thickest at the centre, which is at Niger republic.
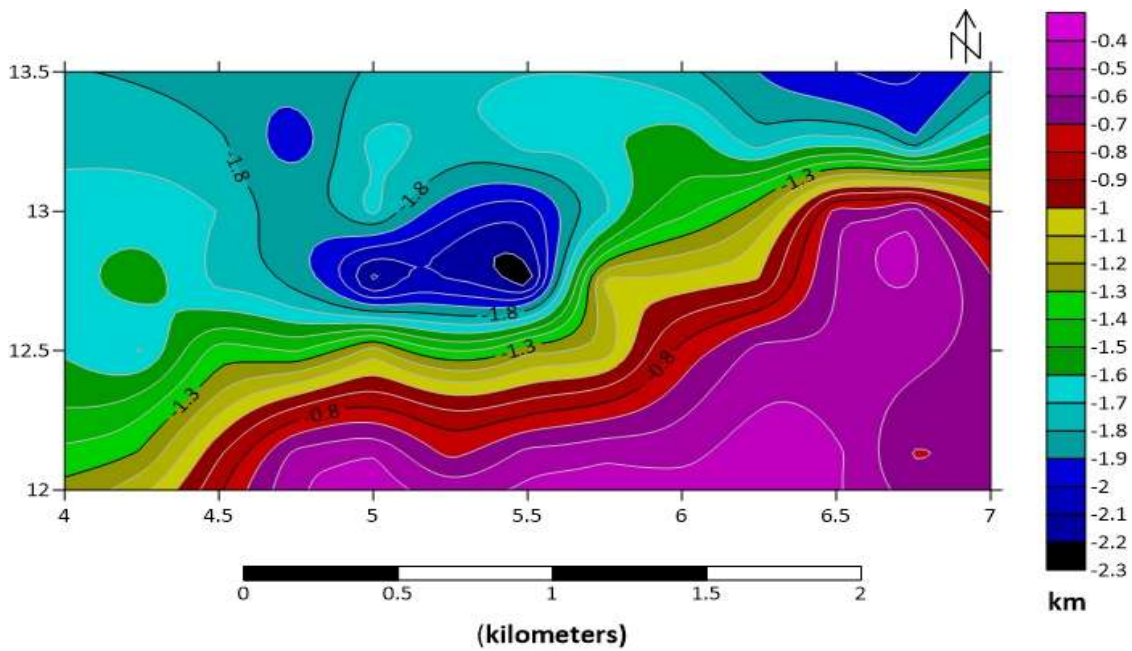
Deeper depth contour map
Fig 8. The deeper depth contour map of the study area

Figure 9, is the deeper depth 3D surface map of the study area. The surface shows the variation in depth of the magnetic source rocks. The sink shows areas where sedimentation is relatively higher. Two prominent sedimentary reservoirs are observed in north east and north central part of the map.
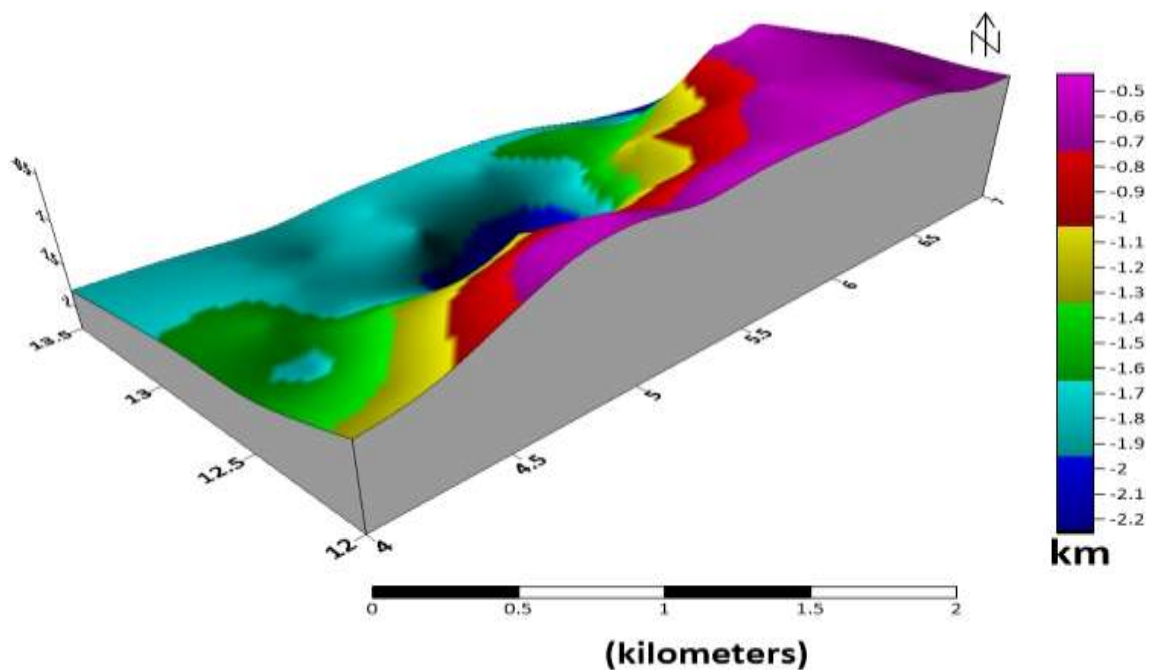
Deeper depth 3D surface map
Fig 9. The deeper depth 3D surface map of the study area

IV. CONCLUSIONS

The high-resolution aeromagnetic data of Sokoto basin has been analyzed and interpreted quantitatively using spectral analysis as depth estimating technique to estimate the thickness of sedimentation for hydrocarbon maturation and accumulation for petroleum exploration in the study area. The following conclusions can be drawn from this study:

1. Spectral analysis indicates that the basin is characterized by shallow and deeper sediments thickness. It is observed that the deeper depth ranges between 0.4 - 2.27km while the shallow depth ranges between 0.12 - 0.4km of the study area respectively.

2. The depth estimating technique used in this study has revealed a sedimentary pile of less than 3.0 km, which might not be sufficient for hydrocarbon maturation and accumulation in the study area. Area with shallow thickness of sediments, could not allow thermal maturation of the sediments, since temperature increase with depth. Depth of 3 km and above has a temperature range of 60˚C and above. According to Nwako L.I (2007), oil window varies between 60˚C and 120˚C, above the temperature of 120˚C the oil may be thermally cracked to gas, and bellow 60˚C, it will form kerogen. Therefore areas with sediment thickness from 3 km and above could be good potential sites for hydrocarbon exploration.

REFERENCES

[1]. Aderoju, A. B., Ojo, S. B., Adepelumi, A. A., & Edino, F. (2016). A reassessment of hydrocarbon prospectivity of the chad basin, Nigeria, using magnetic hydrocarbon indicators from highresolution aeromagnetic imaging. Ife Journal of Science, 18(2), 503-520.

[2]. Adetona, A.A., and Abu, M. (2013). Estimating the thickness of sedimentation within Lower

[3]. Benue Basin and Upper Anambra Basin, Nigeria, using both spectral depth determination and source parameter imaging. ISRN Geophysics, Pp. 1-10.

[4]. Adewumi, T., Salako, K. A., Akingboye, A. S., Muztaza, N. M., Alhassan, U. D., & Udensi, E. E. (2023). Reconstruction of the subsurface crustal and radiogenic heat models of the Bornu Basin, Nigeria, from multi-geophysical datasets: Implications for hydrocarbon prospecting. Advances in Space Research, (71) 4072–4090. https://doi.org/10.1016/j.asr.2023.01.007.

[5]. Adewumi, T., Salako, A. K., Muztaza, N. M., Alhassan, U. D., & Udensi, E. E. (2022). Mapping of subsurface geological structures and depth to the top of magnetic basement in Bornu Basin and its environs, NE Nigeria, for possible hydrocarbon presence. Arabian Journal of Geosciences, 15(18), 1521

[6]. Adewumi, T., Salako, K. A., Usman, A. D., & Udensi, E. E. (2021). Heat flow analyses over Bornu Basin and its environs, Northeast Nigeria, using airborne magnetic and radiometric data: implication for geothermal energy prospecting. Arabian Journal of Geosciences, 14, 1-19.

[7]. Adewumi T, Salako K.A, Adediran O.S., Okwoko O.I., Sanusi Y. A (2019) Curie point Depth and Heat Flow Analyses over Part of Bida Basin, North Central Nigeria using Aeromagnetic Data. Journal of Earth Energy Engineering Vol. 8 No. 1.

[8]. Annual Statistical Bulletin 2019, www.opec.org/opec_web/en accessed on 10/12/2019.

[9]. Bazoobandi MH, Arian MA, Emami MH, Tajbakhsh G, Yazdi A (2016) Petrology and Geochemistry of Dikes in the North of Saveh in Iran, Open journal of marine science 6(02): 210-222.

[10]. Bonde, D.S., Udensi, E.E., and Rai, J.K. (2014) Spectral Depth Analysis of Sokoto Basin. Journal of Applied Physics , 6, 15-21.

[11]. Branson, D.O. (1950). Blackfoot Field, Anderson County, Texas: Bull., Am. Assn. Petro Geo!,34, 1750-1755.

[12]. Bruno, L., Roy, D. L., Grinsfelder, G. S., and Lomando, A. J., 1991, Alabama Ferry Field U.S.A., East Texas Basin, Texas. Bull., Am. Assn. Pet. Geol. 75, 389–408.

[13]. Darnely AG, Ford KL 1989. Regional airborne gamma –ray surveys, a review. In: Garland GD, Edited by. Proceedings of Exploration, 87; Third Decennial Inter –national Conference on Geophysical and Geochemical Exploration for Minerals and Groundwater; Ontario, Canada: data for use in petroleum reconnaissance. Geophysics 59, 411–419.

[14]. Dobrin, M. B. (1976). Introduction to Geophysical Prospecting, 3rd edn., Mc-Graw Hill Books Co., NY, p. 630.Elizabethan Publishing Co., 331-338.

[15]. El-Sadek MA (2002) Application of thorium-normalized airborne radio-

spectrometric survey data of Wadi Araba area, Northeastern Desert, Egypt, as a guide to the recognition of probable subsurface petroleum accumulations. Applied Radiation Isotope 57:121–130.

[16]. El-Sadek, M.A., Ammar, A.A., Omraan, M.A. and Abuelkeir, H.M., 2007: Exploration for hydrocarbon prospects using aerial spectral radiometric survey data in Egypt. Kuwait Journal of Science Engineering, V. 34, No. (2A), pp. 133–160.

[17]. Galbraith, J. H., and Saunders, D. F. (1983). Rock classification by characteristics of aerial Gamma-ray measurements: J. Geochem. Exp!, 18,47-73. Geological Survey of Canada Special V.3. p. 229–240. Geophysics 58 (10), 1417–1427.

[18]. Gingrich, J. E., and Fisher, J. C., (1976). Uranium exploration using the track etch method, Proc., Exploration for uranium ore deposits, Internat. Atomic Energy Agency, 213-227.

[19]. Hahn, A., Kind, E. G., and Mishra, D. C. (1976). Depth estimates of magnetic sources by means of Fourier amplitude spectra. Geophy. Prosp., 24: 278-308.

[20]. Kiran., K. T. (2002). 2D and 3D land Seismic Data Acquisition and Seismic Data Processing. Shell Petrophysics Training Manual. 45-90.

[21]. Kisswani, Khalid, M., (2009). "Economics of oil prices and the role of OPEC. Doctorate Dissertations. AA13367363. https://opencommons.uconn.edu/dissertations/ AA13367363

[22]. Kogbe, C.A Geology of Nigeria, Elizabeth pub.co, Lagos (1976), pp.337-353.

[23]. Kogbe, C.A. (1976) Outline of the Geology of Illummeden Basin, Geology of Nigeria.

[24]. Lawal TO, Nwankwo LI (2014). Wavelet analysis of high resolution aeromagnetic data over part of Chad Basin, Nigeria. Ilorin Journal of Science 1:110-120.

[25]. Mazadiego L (1994) Desarrollo de Una Metodologia Para La Prospecting Geoquimica En Suoerficie de Combustible Fosiles. Tesis de Doctorado. Madrid: 1-353.

[26]. Mollai M, Dabiri R, Torshizian HA, Pe-Piper G, Wang W (2019) Cadomian crust of Eastern Iran: evidence from the Taph Tagh granitic gneisses, International Geology Review,1-21.

[27]. Nigerian Geology Survey Agency. (1976). Geology Map of Nigeria, Scale 1:2,00 000. Geology Survey of Nigeria, Kaduna, Nigeria (Oasis Montaj Software Inc.).

[28]. Nwankwo, L.I., Shehu, A.T. (2015). Evaluation of Curie-point depths, geothermal gradients and near-surface heat flow from high-resolution aeromagnetic (HRAM) data of the entire Sokoto Basin, Nigeria. J Volcanol Geotherm Res 305:45–55.

[29]. Nwankwo, L.I., (2017). Estimation of depths to the bottom of magnetic sources and ensuing geothermal parameters from aeromagnetic data of Upper Sokoto Basin, Nigeria. Geothermics54, 76–81 (81. http://dx.doi.org/10.1016/j.geothermics.2014.12.001).

[30]. Obaje., N. G. (2009). Geology and Mineral Resources of Nigeria. Springer-Verlag Berlin Heidelberg.

[31]. Obaje, N. G; M. Aduku and I. Yusuf , 2013. The Sokoto Basin of Northwestern Nigeria: A Preliminary Assessment of the Hydrocarbon Prospectivity. Journal of Canadian Petroleum Technology.

[32]. Ofor Ngozi. P., Udensi. Emmanuel. E. (2014). Determination of the Heat Flow in the Sokoto Basin, Nigeria using Spectral Analysis of Aeromagnetic Data. Journal of Natural Sciences Research, Vol.4, No.6. 2014.

[33]. Oppenheim, A. V., and Schafer, R. W. (1975). Digital Signal Processing Practice, Hall International Inc., New Jersey, pp. 1227-1296.

[34]. Reeves, C. (2005). Aeromagnetic Surveys; Principles, Practice and Interpretation, Training Programme, NGSA, Nigeria.

[35]. Saunders, D.F. (1989). Simplified evaluation of soil magnetic susceptibility and soil gas hydrocarbon anomalies: Bull., Assn. Petro Geochemical Explorationist, 5, 30-48.

[36]. Saunders, D.F., Burson, K.R., and Thompson, C.K.(1991). Relationship of soil magnetic susceptibility and soil gas hydrocarbon measurements to subsurface petroleum accumulations: Bull., Am. Assn. Petr. Geol., 75, pp. 389-408.